

## Geochemistry and Tectonomagmatic Setting of the Intrusive Rocks in the Hezarkhani Area (Northeast Sonqor, West Iran)

*Frahad Aliani, Soraya Dadfar, Mohammad Maanijou and Mirmohammad Miri*

Departeman of Geology, Bu-Ali-Sina University, Hamedan, Iran

**Abstract:** The plutonic bodies in the northeast of the Sonqor area compose a small part of the Sanandaj-Sirjan zone. According to the field and microscopic observations, the study area is composed of two major unites; intermediate and felsic. Mineralogical and geochemical studies show that these rocks are I-type, calk-alkaline and metaluminous. The regular variation trends in the incompatible elements diagrams demonstrate that these rocks generated by fractional crystallization process. The low  $(Al_2O_3)/(FeO+MgO+TiO_2)$  and  $(Na_2O+K_2O)/(FeO+MgO+TiO_2)$  ratios together with REE and trace elements evidences such as enrichment in Th, Rb, La, Ce, Nd and depletion in Ti and Eu, A/(NK) values  $> 1$  and A/(CNK) values  $< 1$  and this ration, Rb/Sr is less than 0.6 indicate that their initial magma is generated from the lower crust. Discrimination diagrams for tectonic setting, Th/Ta ratio in the range of (6-20) and enrichment in LILEs and LREE relative to HFSEs and HREE, all of this evidence are indicate the intrusion of this body into the subduction zone related to an active continental margin setting, that according to geological history of this area, it can be attributed to subduction of Neo-Tethyan oceanic crust below Central Iran.

**Key words:** I-type • Active continental margins • Calk-alkaline • Hezarkhani • Sonqor • Iran

### INTRODUCTION

The study area is situated in the northeast of the Sonqor area (Hazarkhani area) in west Iran with coordinates 34, 54-34, 57 E to 47, 51-47, 54 N (Figure 1). This area belongs to the Sanandaj-Sirjan zone based on the classification of Iran litostructural zones [1]. [2] have determined the age of the plutonic rocks in the study area about 40 billion years, through K-Ar method. [3] and [4], also have studied the plutonic bodies in the Sonqor area. However, the plutonic rocks of the Hazarkhani area has not been studies especially. The aim of the present paper is to study the geochemistry and petrology of the plutonic rocks in this area. The study area can be divided to the two general units (intermediate and felsic) that all of these rocks are calk-alkaline and metaluminus generated by fractional crystallization. Also REE and trace elements evidences indicate that these are formed by metaluminous I-type magmatism in an active continental margin and generated through lower crust partial melting during a subduction process.

**The Study Method:** All samples of the plutonic rocks in the study area were studies by polarized cross-light microscope. Five of these samples with minimal effects of hydrothermal alteration were selected for whole-rock geochemical analysis (Table 1). Major elements and some trace elements (Ba, Sr, Nb, Y, Zn and Zr) analyzed by inductively coupled plasma atomic emission spectroscopy (ICP-AES) method with a lithium metaborate fusion. Other trace elements and REE were determined by inductivity coupled plasma-mass spectrometry (ICP-MS) and lithium metaborate fusion at the SGS laboratory in Toronto, Canada.

**Regional Geology:** The study area in the northeast of the Sonqor area is plutonic rocks located in the northeast of the Hazarkhani village. The rock sequences in the Hazarkhani area are volcano-sedimentary sequence (Sonqor series) comprising of limestone and intermediate to mafic volcanic rocks that are middle to late Jurassic in age [5] and Eocene plutonic rocks [2] limestone and intermediate to mafic volcanic rocks that are middle to late

Table 1: Major and trace element compositions of the representative rocks in the northeast of the Sonqor. (-) means not determined

Samples	Diorite	Monzodiorite	Qz-monzodiorite	Monzonite	Granodiorite
Oxides	Hez14	Hez1	Hez17	Hez8	Hez12
SiO <sub>2</sub>	50.1	52.5	58.9	56.3	71.2
Al <sub>2</sub> O <sub>3</sub>	17.8	19.2	15.6	15.4	14.9
Fe <sub>2</sub> O <sub>3</sub>	9.97			8	1.55
CaO	5.59	6.58	3.93	3.96	0.42
MgO	6.98	2.86	2.33	3.64	1.77
Na <sub>2</sub> O	3.9	5.5	6.7	7.3	7.8
K <sub>2</sub> O	0.34	0.3	0.35	0.32	1.7
Cr <sub>2</sub> O <sub>3</sub>	0.02	-	-	-	-
TiO <sub>2</sub>	1.47	1.79	1.98	2.29	0.55
MnO	0.16	0.1	0.08	0.09	-
P <sub>2</sub> O <sub>5</sub>	0.21	0.72	0.55	0.57	0.17
LOI	3.33	1.33	1.86	1.32	0.96
A/CNK	1.1	0.91	0.85	0.86	0.96
A/NK	1.3	1.3	2.1	2	1.3
Mg#	56.2	44.8	42.5	48.2	49.8
K <sub>2</sub> O/Na <sub>2</sub> O	0.010	0.045	0.052	0.005	0.0205
Sum	102.2	99.3	98.9	99.1	99.5
Ba	110	720	110	90	369
Ce	32.5	153	105	103	94.1
Cs	1	1.8	0.3	0.5	0.1
Cu	102	13	27	20	7
Dy	4.89	8.32	10.2	8.95	6.04
Er	2.87	4.37	6.25	5.31	3.71
Eu	1.42	3.25	2.42	2.17	1.11
Gd	4.28	9.42	9.53	8.76	5.35
Lu	0.37	0.56	0.97	0.69	0.65
Nb	8	54	41	34	47
Nd	15.1	59.6	45.7	41.9	35
Rb	4.9	42	9	9.2	30
Sm	4.1	10.4	9.8	9	6.7
Sr	245	570	200	130	80
Ta	-	1.9	0.8	3.5	3.7
Tb	0.77	1.46	1.65	1.4	0.93
Th	1.5	10.1	14.6	11.7	31
Tm	0.4	0.62	0.97	0.76	0.61
U	0.36	2	3.11	3.29	6.91
Co	38.4	9	4.8	14.4	7
Ga	18	22	24	24	21
Hf	3	4	9	7	8
Ho	1.03	1.68	2.19	1.84	1.28
La	10.6	85.1	55.1	55.9	39.4
Pr	3.28	16.5	12.1	11.2	10.3
Sn	-	3	4	5	9
V	250	141	176	210	43
Y	24.7	2	3	4	31.8
Yb	2.6	3.9	6.1	4.9	4.3
Zn	110	160	380	280	320
Zr	107	155	265	263	304
Eu/Eu*	0.51	0.69	0.77	0.75	0.57
Th/Ta	-	6.3	6.51	6.48	8.38
Rb/Sr	0.05	0.07	0.09	0.07	0.08

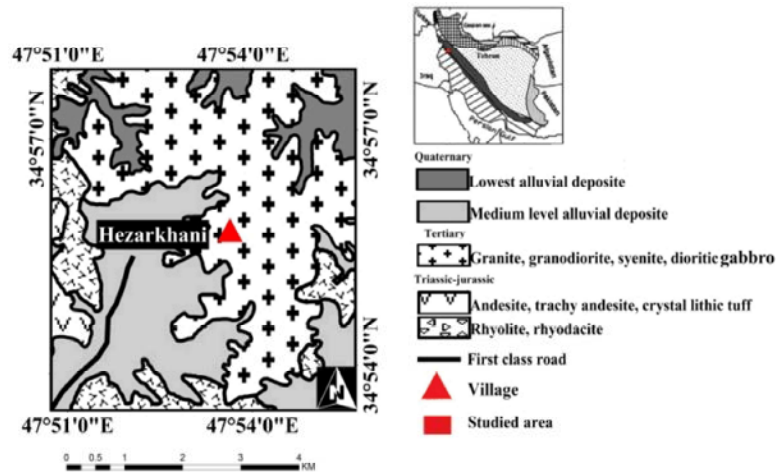


Fig. 1: Geological map of the Northeast Sonqor. Modified from geological map of Sonqor [5].

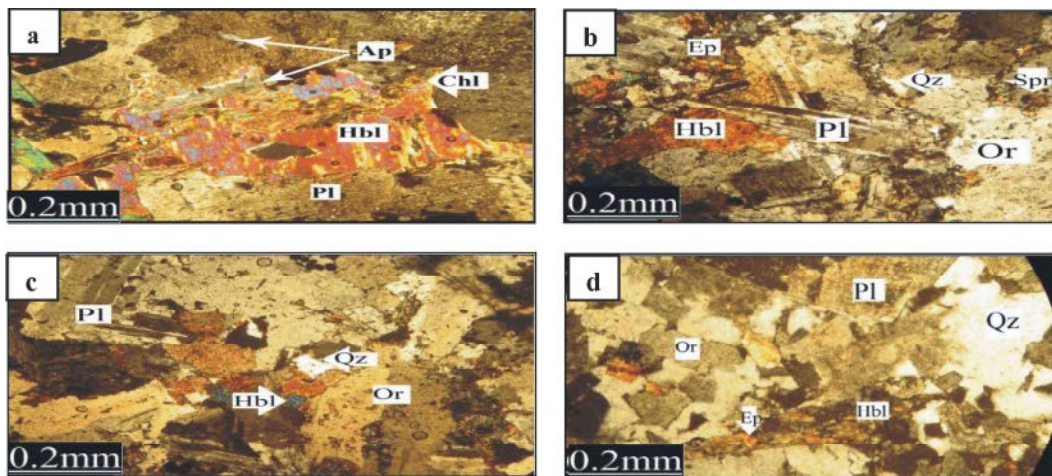


Fig. 2: (a). Pegmatoid texture in the pegmatitic diorite, with alteration of hornblende to chlorite. (b). Subhedral to anhedral granular texture in the monzodiorite with plagioclase, hornblende and orthoclase. (c). Photomicrograph of the monzonite. (d). Photomicrograph of the granodiorite. Abbreviation of minerals are Hbl: Hornblende, Pl: plagioclase, Sph: sphene, Ep: Epidote, Chl: Chlorite [6].

Jurassic in age and Eocene plutonic rocks [2] which intercrossed the Triassic-Jurassic volcano-sedimentary sequence [5] in the area (Figure 1).

**Petrography:** According to the petrographic studies, the plutonic rocks in the study area comprising of intermediate and felsic units.

**The Intermediate Unite:** This unite is visible in the Hazarkhani area heights with NW-SW trends. This unite is composed of intermediate rocks such as diorite (pegmatitic diorite and microdiorite), monzodiorite, quartz-monzonite and monzonite. Subhedral to anhedral granular are the general textures. However, pegmatoid, intergranular, poikilitic (hornblende crystals in plagioclase

and vice versa), microgranular and perthitic textures are visible in some samples. These rocks composed of plagioclase (50-55%), hornblende (35-45%), orthoclase (5-10%), quartz (<10%) and clinopyroxene (0-7%) as the main minerals. The accessory minerals are apatite, sphene and opaque minerals. Zoisite, clinozoisite, epidote and clay minerals are secondary minerals that resulting from the plagioclase and orthoclase alteration. Also chlorite is other secondary minerals which resulted from hornblende alteration (Figure 2a, b, c).

**The Felsic Unite:** This unite is composed granodiorite rocks and crops out in the northeast of the Hazarkhani (small size outcrops and in contact with intermediate rocks) areas. These rocks are dark to light green,

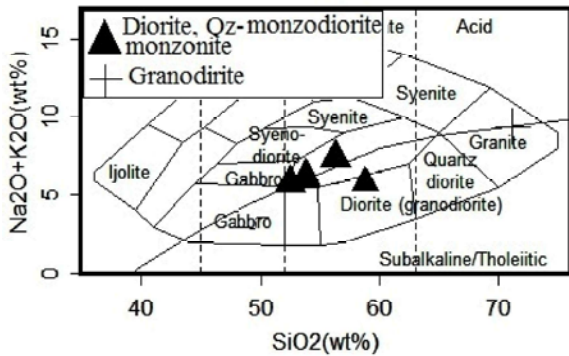


Fig. 3: Total alkali (Na<sub>2</sub>O+K<sub>2</sub>O) vs. silica diagram for geochemical classification of the studied samples.

medium to fine grained and leucocratic. The general textures in these rocks are subhedral to anhedral granular. Also, porphyroid texture (with plagioclase phenocrysts) in the tonalits and peritic and poikilitic textures in the granodiorites are visible. The main minerals of these rocks are plagioclase (60-65%), quartz (25-30%) and orthoclase (<10% in the tonalities and <20% in the granodiorites). Accessory minerals are sphene, apatite (as needle crystal inclusions in quartz and orthoclase). Secondary minerals are epidote, clay minerals and sericite resulting from the plagioclases and orthoclases (Figure 2d).

**Geochemistry:** As mentioned above, five samples from the Hazarkhani area were analyzed by ICP-MS and ICP-AES methods (Table 1). The SiO<sub>2</sub>-(Na<sub>2</sub>O+K<sub>2</sub>O) diagram [7] is used for geochemical classification of these samples (Figure 3). As visible the samples plot within granite and sienodiorite fields (Figure 3) that are compatible with petrography results.

Major and trace elements versus SiO<sub>2</sub> variation diagrams (Harker diagrams) are useful in petrological interpretations [8]. Major elements Harker diagrams are represented in Figure 4. In these diagrams MgO, MnO, Fe<sub>2</sub>O<sub>3</sub>, Al<sub>2</sub>O<sub>3</sub>, CaO and TiO<sub>2</sub> decrease with SiO<sub>2</sub> contents increasing. Also K<sub>2</sub>O and Na<sub>2</sub>O increase with SiO<sub>2</sub> contents increasing. Because MgO, MnO, Fe<sub>2</sub>O<sub>3</sub> and TiO<sub>2</sub> take part in ferromagnesian and titanium-bearing minerals formation in initial steps of crystallization, decrease with increasing in SiO<sub>2</sub> contents. The negative correlation of Al<sub>2</sub>O<sub>3</sub> and CaO is because of their participation in plagioclase formation. Because plagioclase and orthoclase crystallize in final steps of magma evolution, K<sub>2</sub>O and Na<sub>2</sub>O decreased.

Trace elements Harker diagrams are shown in Figure 5. As visible, Rb, Ba, Th and U increase and V and Sr decrease with SiO<sub>2</sub> contents increasing (Figure 5).

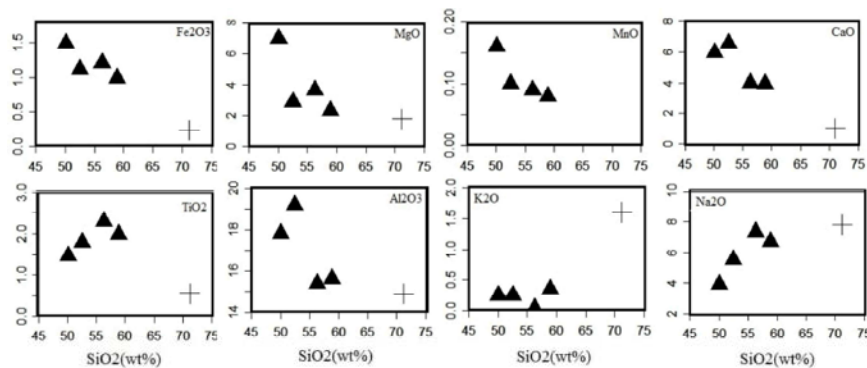


Fig. 4: Major elements Harker diagrams for the studied samples. Symbols as in Figure 3.

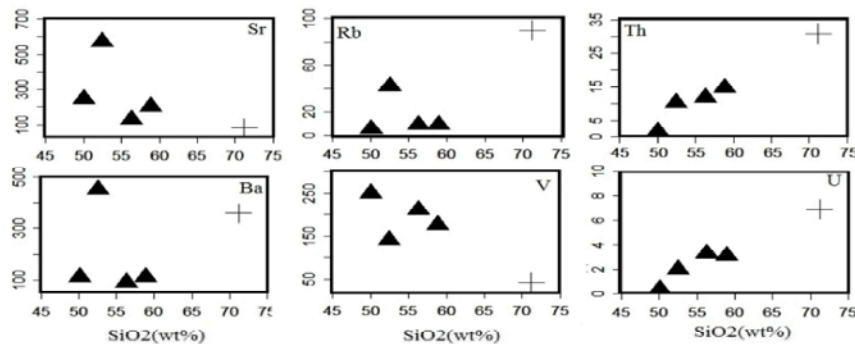


Fig. 5: Trace elements Harker diagrams for the studied sample. Symbols as in Figure 3.

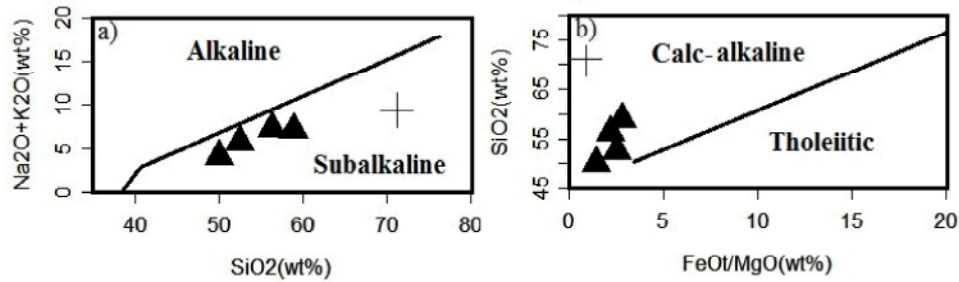


Fig. 6: (a). Total alkalis vs. silica diagram [9]. (b). (FeO<sub>tot</sub>/MgO) vs. silica diagram, for separating calcalkaline and tholeiitic magmas [10], samples are plotted in the range of calcalkaline and sub-alkaline magmas. (Symbols as in Figure 3).

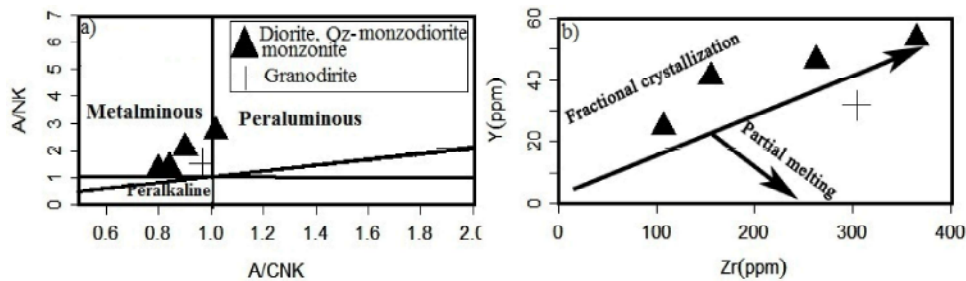


Fig. 7: (a) A/CNK vs. A/NK variation diagram with metaluminous, peraluminous and peralkaline fields [11]. Most of the studied samples plot within metaluminous field. (b) Y vs. Zr diagram [13] which indicates the studied sample generated by fractional crystallization process.

Rb and Ba take part in orthoclase in final steps of crystallization and thus increase. Sr also participates in Ca-plagioclase in initial steps and decrease in final steps. Th is an incompatible element and thus cannot participate in silicate minerals and Th enriched in magma. Vanadium is a compatible element and thus in the beginning of the fractionation process separated from the magma and entered to the minerals such as pyroxene and magnetite causing to decrease in final steps. In the (Na<sub>2</sub>O+K<sub>2</sub>O) versus SiO<sub>2</sub> diagram [9] and the (Fe<sub>tot</sub>/MgO) versus SiO<sub>2</sub> diagram [10], all the samples plot within calc-alkaline field (Figure 6a, b). In the (Na<sub>2</sub>O+K<sub>2</sub>O) versus SiO<sub>2</sub> diagram [9] and the (Fe<sub>tot</sub>/MgO) versus SiO<sub>2</sub> diagram [10], all the samples plot within calc-alkaline field (Figure 6a, b).

Degree of alumina saturation is shown in a plot of molar A/CNK vs. A/NK (Figure 7a). In this diagram most of the sample have A/NK= (1.3-2.1) and A/CNK= (0.85-1.1). Most of the sample plotting in the metaluminous field and some plot near peraluminous field [11] (Figure 7a). The presence of mafic minerals such as hornblende and pyroxene in the studied sample and also the lack of Al-enriched minerals like cordierite, corundum and topaz in these rocks are indicators for the metaluminous nature of the studied samples.

Whereas both partial melting and fractional crystallization processes would lead to similar final effects in forming of magmatic rocks [12], therefore by observing affinity relations in the samples, it is needed to realize that what process is cause of these relations. Therefore the diagram of Y-Zr [13] has been applied to examine the probable relation between samples (Figure 7b). By referring to this diagram, probable process in forming region's intrusive rocks is fractional crystallization. The result from this diagram agrees with relative regular trends in the Harker diagram (Figure 4 and 5) which indicate the performance of fractional crystallization process in generation of the plutonic rocks in the study area.

**Rare Elements Geochemistry:** Chondrite-normalized multi-element variation diagrams for the studied samples [14] are shown in Figure 8a. In these diagrams, the abundance of rare elements in felsic, intermediate units is similar and all of samples show enrichment in LILE and depletion in HFSE (Y, Yb, Sm, Zr, Hf, Ta, Nb). enrichment in LILEs (Th, Rb) relative to HFSEs (Y, Yb, Sm, Zr, Hf, Ta, Nb) (Figure 8a) could be resulted from a low-degrees partial melting in mantle origin, the movement of elements during alteration process, the role of metasomatism mantle, the contamination by crustal

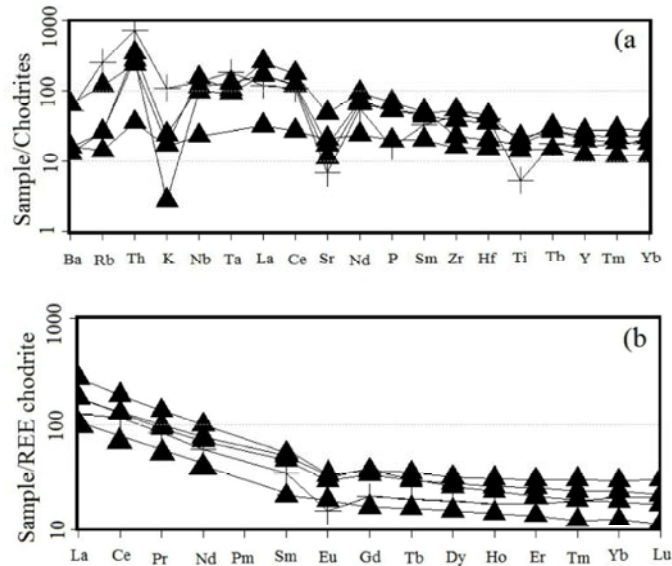


Fig. 8: (a). Chondrite-normalized multi-element variation diagrams for studied samples. All samples are normalized by values of [14]. (b). Chondrite-normalized REE patterns for studied samples. All the samples are normalized by [19] values. Symbols as in Figure. 7.

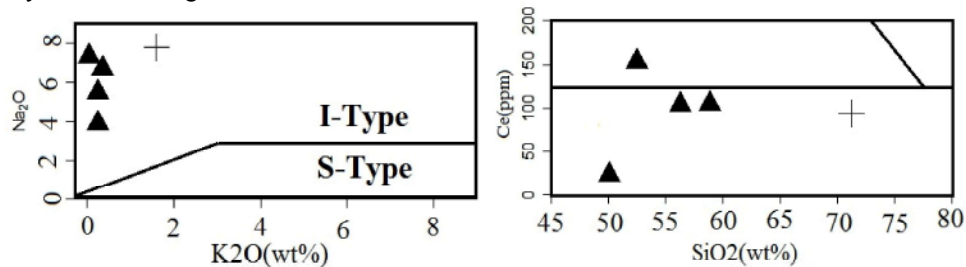


Fig. 9: (a).  $\text{Na}_2\text{O}$  vs.  $\text{K}_2\text{O}$  variation diagram [20], for separating I and S type granites. (b) Ce vs.  $\text{SiO}_2$  diagram [21], for separating of I- and A-type granite.

materials, or interference of crust in forming region's rocks [15-17]. Of course Sr shows depletion, likely due to segregation of plagioclase as the initial phase in the mafic unit. Also the presence of Ti in titanium-bearing minerals such as ilmenite in the mafic unit, thus by segregation of these elements, causing negative anomaly [18].

Chondrite-normalized rare earth element (REE) patterns [19] are shown in Figure 8 b. All of the samples show light rare earth element (LREE) enrichment relative to heavy REE (HREE). According to the Figure 8b intermediate and felsic ( $\text{Eu}/\text{Eu}^* = 0.51-0.77$ ) units have negative Eu anomalies (Table 1). Eu anomalies in the studied samples likely were caused by the fractional crystallization of plagioclase during magma crystallization process. Based on [20] enrichment in LILEs and LREE relative to HFSEs and HREE, indicating intrusion of magma into the subduction zone related to an active continental margin setting.

**Tectonic Setting and Petrogenesis:** Based on the abundance of rare and major elements, it is tried here to examine tectonic sitting and magmatic origin of the studied samples.  $\text{Na}_2\text{O}$  versus  $\text{K}_2\text{O}$  variation diagrams [21] are applied for separating of I- and S-type granites (Figure 9a) and also Ce versus  $\text{SiO}_2$  diagram [22] is used for separating of A-type granite from I-type granite (Figure 9b). It could be noted that by referring to these diagrams, the studied rocks plot within the I-type granite field. Some proofs such as the presence of various rocks in this region including granodiorite, monzonite, monzodiorite, quartz monzodiorite, diorite the presence of hornblende, magnetite, apatite and sphene and the lack of metamorphic minerals such as garnet, polymorphs of aluminosilicate and cordierite and the lack of corundum in norm, the ratio  $(\text{K}_2\text{O}/\text{Na}_2\text{O}) > 1$ ,  $(\text{K}_2\text{O}/\text{Na}_2\text{O}) = 0.17$ , to have metaluminous characteristic [21], ascendant trend in Th- $\text{SiO}_2$  [23] are indicatives for the presence of I type granites in the region.

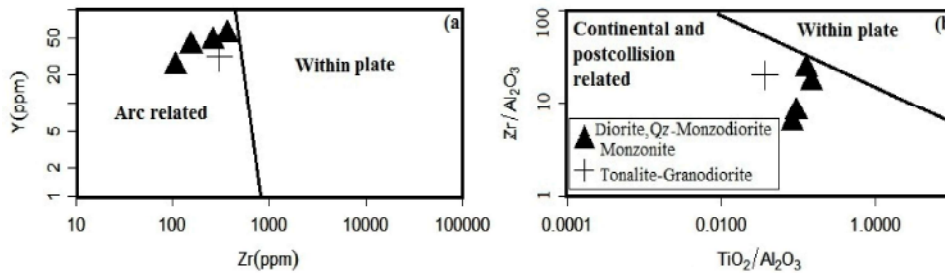


Fig. 10: (a,b). Zr/Al<sub>2</sub>O<sub>3</sub> vs. TiO<sub>2</sub>/Al<sub>2</sub>O<sub>3</sub> and Zr vs. Y variation diagrams [23].

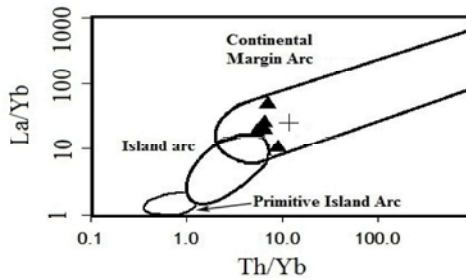


Fig. 11: Th/Yb vs. La/Yb [24] to determine tectonic sitting of studied sample. Symbols as in Figure 10.

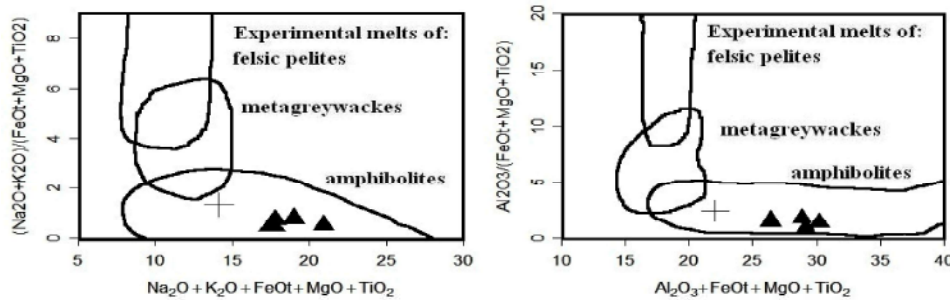


Fig. 12: The fields on the diagram are chemical composition of melts from experimental studies of partial melting felsic pelites, metagreywackes and amphibolites [29-31] and samples of the studied area. Symbols as in Figure 10.

The Y versus Zr and Zr/Al<sub>2</sub>O<sub>3</sub> versus Ti<sub>2</sub>O<sub>3</sub>/Al<sub>2</sub>O<sub>3</sub> diagrams [24] (Figure 10a, b) and also Th/Yb versus La/Yb diagram [25] (Figure 11) are used to determine the tectonic setting of the studied samples. In the northeast of the Sonqor area, as pointed out in (Figure 10a, b and 11) intermediate and felsic samples plot in the continental margin tectonic setting field. Based on [26] in the subduction zone the amount of Th increases and Th/Ta ratio in the subduction-related rocks in active continental margin varies in the range of (6-20 ppm). This ratio in the studied samples (ave., 9.4) is consistent with a subduction zone.

**Origin of the Plutonic Rocks:** By considering contents of SiO<sub>2</sub> (average: 50-70 percent), #Mg less than 60 (Table 1) and low values of transition elements Ni, Cr, Co and V in the studied samples, the probability of their direct origination from the mantle can be rejected [18,27].

According to the geochemical evidences such as enrichment in Th, Rb, La, Ce, Nd and depletion in Ti and Eu, A/(NK) values > 1 and A/(CNK) values < 1 and Rb/Sr < 0.6 which points to partial melting of lower crust sources [28], thus we can expect magmatic sources from lower crust sources partial melting.

According to results of partial melting in crustal rocks, I type calcalkaline granitoid magmas can be derived from partial melting of mafic to hydrous intermediate metamorphic rocks in the crust [29]. Beside it, lavas derived from partial melting of mafic sources have lower proportions of (Al<sub>2</sub>O<sub>3</sub>)/(FeO+MgO+TiO<sub>2</sub>) and (Na<sub>2</sub>O+K<sub>2</sub>O)/(FeO+MgO+TiO<sub>2</sub>) relating to lavas resulted from metapelite melting (Figure 12). Therefore, intrusive rocks with lower proportions of (Na<sub>2</sub>O+K<sub>2</sub>O)/(FeO+MgO+TiO<sub>2</sub>) and Al<sub>2</sub>O<sub>3</sub>/(FeO+MgO+TiO<sub>2</sub>) could be derived from crustal rocks. In drawn diagrams based on empirical studies

[30,31,32], mafic samples as initial magma composition are presented in the combined area of empirical lavas derived of metaplates, metagreywackes and amphibolites melting (Figure 12). Partial melting in metamorphosed igneous rocks (intermediate) in lower crust can lead to tonalite (diorite) magmas formation [33]. It seems that the granitoid rocks in the northeast of the Sonqor area have been formed by partial melting of lower crust protoliths.

### CONCLUSION

Plutonic complex in the north east of the Sanqor area contains different rock units. The variety of rocks in this region ranges from diorite to granodiorite. According to the mineralogical, petrological and geochemical studies, the rocks of this suite geochemically are I-type, low-K calc-alkaline and metaluminous. Trends of compatible elements indicate the important role of fractional crystallization in the genesis of these rocks. The low  $Al_2O_3/(FeO+MgO+TiO_2)$  and  $(Na_2O+K_2O)/(FeO+MgO+TiO_2)$  ratios, enrichment in Th, Rb, La, Ce, Nd and depletion in Ti and Eu, A/(NK) values > 1 and A/(CNK) values < 1 and Rb/Sr < 0.6 shows that the origin of the initial magma is from the lower crust that created in a subduction tectonic setting. Discrimination diagrams for tectonic setting, Th/Ta ratio in the range of (6-20) and enrichment in LILEs and LREE relative to HFSEs and HREE, indicate the intrusion of this body into the volcanic arc related to an active continental margin setting, so that with regard to geological history of this area, it can be attributed to subduction of Neo-Tethyan oceanic crust below Central Iran.

### REFERENCES

1. Mohajjel, M., 1997. Structure and tectonic evolution of Paleozoic-Mesozoic rocks, Sanandaj-Sirjan Zone, western Iran. Unpublished Ph.D. Thesis, University of Wollongong, Wollongong, Australia.
2. Braud, J. and H. Bellon, 1975. Donnees nouvelles sur le domaine metamorphique de Zagros (Zone de Sanandaj-Sirjan) au niveau de Kermanshah-Hamedan (Iran): nature, age et interpretation des series metamorphiques et des intrusion, evolution structural. *Eclog. Helvet.*
3. Braud, J. and A. Aghanabati, 1978. 1:250000 Geological map of Kermanshah, Geological Survey and Mining of Iran.
4. Miri, M., 2011. The petrological and geochemical studies of igneous rocks of Takye Bala area (southeast of Kurdistan) with speatial view on the iron mineralization, Master of Science Thesis, Bu Ali Sina University. Hamedan, Iran.
5. Eshraghi, S.A., M.B. Jafarian and B. Eghlimi, 1996. 1:100000 Greological map of Sonqor, Geological Survey of Iran.
6. Withney, D. and W.D. Evance, 2010. Abbreviations for names of rock-forming minerals. *American Mineralogist*, 95: 185-187.
7. Cox, K.G., J.D. Bell and R.J. Pankhurst, 1979. *The Interpretation of Igneous Rocks*, Allen and Unwin, London, pp: 450.
8. Harker, A., 1997. *The natural history of igneous rocks*. Methuen: London.
9. Irvine, T.N. and W.R.A. Baragar, 1971. Guide to the chemical classification of the common volcanic rocks. *Canadian Earth Science*, 8: 523-545.
10. Miyashiro, A., 1974. Volcanic rock series in island arcs and active continental margins, *American journal of Science*, 274: 321-355.
11. Shand, S.J., 1943. *Eruptive rocks*, T. Murby, London.
12. Ghasemi, H., A. Ramazani and A. Khanalizadeh, 2007. Petrology, Geochemistry and Tectonomagmatic Setting of the Silijerd Intrusion, Northwest Saveh, *Earth sience*, 17(67): 68-85.
13. Abdalla, J.A., A. Said and D. Visona, 1997. New geochemical and petrographic data on the gabbro-syenite suite between Hargeysa and Barbera sheikh (Northern Somalia). *African Erath Science*, 23(2): 363-373.
14. Thompson, A.B., 1982. Magmatism of the Bristish Tertiary Volcanic Province, Scotlandian. *Geology*, 18: 50-107.
15. Rogers, N.W., C.J. Hawkesworth and D.S. Ormerod, 1989. Late Cenozoic basaltic magmatism in the Western Great Basin California and Nevada. *Geophysics Research*, 100: 10287-10301.
16. Floyd, P.A. and J.A. Winchester, 1975. Magma type and tectonic setting discrimination using immobile elements. *Earth and Planetary Science Letters*, 27: 211-218.
17. Sajona, F.G., R.C. Maury, H. Bellon, J. Cotton and M. Defant, 1996. High field strength elements of Pliocene-Pleistocene island-arc basalts Zamboanga Peninsula, Western Mindanao (Philippines). *Petrology*, 37: 693-726.



18. Wilson, M., 1989. *Igneous Petrogenesis*. Unwin Hyman, London.
19. Boynton, W.V., 1984. Geochemistry of the rare earth elements: meteorite studies. In: Henderson P. (ed.). *Rare earth element geochemistry*, Elsevier, pp: 63-114.
20. Fitton, J.G., D. James, P.D. Kempton, D.S. Ormerod and W.P. Leeman, 1988. The role of lithospheric mantle in the generation of Late Cenozoic basic magmas in the western United States. *Petrology, Special Ithosphere*, pp: 331-349.
21. Chappell, B.W. and A.J.R. White, 1992. I-and S-type granites in the Lachlan Fold Belt, Royalal Society of Edinburgh. *Earth Sciences*, 83: 1-26.
22. Collins, W.J., S.D. Beams, A.J.R. White and B.W. Chappell, 1982. Nature and origion of A type granites with particular refrence to south-eastern Australia, *Contrib. Mineral, Petrology*, 80: 189-200.
23. Chappell, B.W., C.J. Bryant, D. Wyborn, A.J.R. White and I.S. Williams, 1998. High and low Temperature I-type granites. *Resource Geology*, 48: 225-236.
24. Muller, D. and D.I. Groves, 1997. Potassic igneous rocks and associated goldcopper mineralization, *Lecture Notes in Earth Sciense*, pp: 56.
25. Condie, K.C., 1989. Geochemical changes in basalts and andesites across the Archean-Proterozoic boundary: identification and signification and significance. *Litthos*, 23: 1-18.
26. Schandl, E.S. and M.P. Gorton, 2002. Application of high field strength elements to discrimination tectonic settings in VMS environments. *Econmic Geology*, 97: 629-642.
27. Kuster, D. and U. Harms, 1998. Post-collisional potassic granitoids from the southern and northwestern parts of the Late Neoproterozoic East African Orogen: a review. *Lithos*, 45: 177-195.
28. Chappell, B.W. and A.J.R. White, 1974. Two constrasting granite types. *Pacific Geology*, 8: 173-174.
29. Roberts, M.P. and J.D. Clemens, 1993. Origion of high-potassium, calc-alkaline, I-type granitoids. *Geology*, 21: 825-828.
30. Patino Douce, A.E., 1996. Effects of pressure and H<sub>2</sub>O content on the composition of primary crustal melts, *Trans. R.Soc. Edinburgh: Earth Science*, 87: 11-21.
31. Patino Douce, A.E. and J.S. Beard, 1995. Dehydration-melting of biotite gneiss and quartz amphibolite from 3 to 15k bar, *Petrology*, 36: 707-738.
32. Patino Douce, A.E. and T.C. McCarthy, 1998. Melting of crustul rocks during continental collision and subduction, In: *Geodynamics and geochemistry of ultrahigh-pressure rocks, Petrology and Structural Geology*. Kluwer Academic Publishers, Dordrecht, 10: 27-55.
33. Johannes, W. and F. Holtz, 1996. *Petrogenesis and Experimental Petrology of Granitic Rocks*, Berlin, Springer-Verlag.